Powder injection molding of HA/Ti6Al4V composite using palm stearin as based binder for implant material

Amir Arifin [a,b], Abu Bakar Sulong [a,*], Norhamidi Muhamad [a], Junaidi Syarif [a], Mohd Ikram Ramli [a]

[a] Department of Mechanical and Materials Engineering, Universiti Kebangsaan Malaysia, 43600 Bangi, Selangor, Malaysia
[b] Department of Mechanical Engineering, Sriwijaya University, 30662 Indralaya, Sumatera Selatan, Indonesia

A B S T R A C T

Titanium alloy (Ti6Al4V) and hydroxyapatite (HA) are well-known materials applied in implants. Ti6Al4V shows good mechanical properties and corrosion resistance, whereas HA possesses excellent biocompatibility and bioactivity but weak mechanical properties. The combination of the Ti6Al4V and HA properties is expected to produce a superior material for bio-implants. This study aimed to analyze the feasibility of fabricating HA/Ti6Al4V composites through powder injection molding (PIM) using palm stearin as base binder. In this study, 90 wt% Ti6Al4V and 10 wt% HA were mixed with the palm stearin and polyethylene binder system. The HA/Ti6Al4V feedstock showed pseudoplastic properties, suggesting its suitability for PIM. Flexural test revealed that the strength of the sintered composite ranges from 67.12 MPa to 112.97 MPa and its Young's modulus ranges from 39.28 GPa to 44.25 GPa. The X-ray diffraction patterns and energy-dispersive X-ray spectra of the composite showed that the HA decomposed and formed secondary phases. Isotropic porous structure was observed on the sintered sample because of HA decomposition. Results showed that the palm stearin can be used as based binder in fabricating HA/Ti6Al4V composites via PIM. The mechanical properties of the sintered composites are nearly similar to those of the human bone. In addition, the increase in weight of the sintered composite during in vitro tests indicated the nucleation and growth of the Ca–P phase, which exhibited the biocompatibility of the fabricated HA/Ti6Al4V composite.

© 2014 Elsevier Ltd. All rights reserved.

1. Introduction

Powder injection molding (PIM) is combination of plastic injection molding and powder metallurgy, which is suitable in fabricating small and complex parts in large quantities [1]. The PIM process typically consists of four stages: mixing, injecting, debinding, and sintering [2,3]. Hydroxyapatite (HA) shows similar properties to the human bone because of its chemical structure. However, the low mechanical properties of pure HA make it unsuitable for heavy loading applications. Intensive research has been conducted to increase the mechanical properties of HA by modifying the parameters and the routes of the process prior to combining with other materials [4–8]. Titanium and HA are attractive materials for medical application [9]. Titanium alloy has good mechanical yet poor biocompatibility properties. HA is advantageous because it possesses similar chemical structure to the human bone and excellent biocompatibility; HA also enhances growth of natural

tissues. Thus, HA and titanium alloy composite can be a superior material for biomedical implant [10].

Powder metallurgy method is the main option to produce HA/Ti6Al4V composites [6,11]. However, results show that such composites exhibit properties such as mechanical strength, Young's modulus, and pore type that are insufficient for substitution of human bone. The fabrication of HA/Ti6Al4V composite using PIM is rarely reported. Thian et al. [12] produced HA/Ti6Al4V composite using PIM with commercial binder. Results showed that some of the cracks and void are observed on certain places. In the sintered part, cracks that originate from the Ti particles are formed, which is attributed to the varying thermal expansions, thereby inducing residual stress on the composite.

One of the issues of metal implants in terms of mechanical properties is the large difference between the Young's modulus of the metal implants and human bones [13]. Metal implants have higher Young's modulus (105 GPa for titanium alloy) [14] than the cortical bone (10–30 GPa) [15,16]. This remarkable difference in Young's modulus is known as "stress shielding," which is due to the inhomogeneous distribution of stress transfer from bone to metal implant. The presence of porous structure in the implant

---

material reduces the Young's modulus of the metal [16,17]. In the powder metallurgy process, combining two or more powders with different properties, such as powder size, type of powder (e.g., metal and ceramic), and thermal expansion coefficient, is challenging. For example, a difference in particle size increases critical powder loading. In a high powder loading condition, a small quantity of binder is necessary. The binder is important in determining the success of the injection stage in PIM. Moreover, differences in thermal expansion coefficients induce residual stress and crack during and after sintering [12,18].

Palm stearin is derived from palm oil. Palm stearin has been used as component of binder systems [19–21]. As a natural binder, it is environmentally friendly and used as lubricant and surfactant in injection process. Other advantages of palm stearin include providing capillary pores to remove backbone binder during thermal debinding. The main objective of this study is to analyze the feasibility of fabricating HA/Ti6Al4V composite as implant material through PIM with the use of palm stearin as the based binder.

2. Experimental details

Titanium alloy (Ti6Al4V) with an average particle size 19.6 μm and non-calcined HA with an average particle size of 5 μm was used in this study (Fig. 1a and b). The size of the particles was measured using Malvern particle size analyzer. Table 1 shows the distribution of particle size for HA and Ti6Al4V powders, which have D_{50} of 5.3 and 19.6 μm, respectively. The composition of mixture consists of 90 wt% Ti6Al4V and 10 wt% HA. A binder system composed of a mixture of 60 wt% palm stearin and 40 wt% polyethylene was used in this study.

The critical powder volume concentration of the mixture is measured using the oil absorption technique based on ASTM: D-281-12. Pre-mixing process of Ti6Al4V and HA powders were performed for 30 min prior to primary mixing with binder system using Brabender mixer. Powder mixture was mixed with binder system for another 30 min using Brabender mixer at 30 rpm. Firstly, polyethylene was melted completely in mixing machine, then palm stearin and followed by powder mixture of Ti6Al4V and HA. Fig. 2 shows SEM image of the powder mixture of Ti6Al4V and HA after pre-mixing process. The powder loading for this mixing process is 78.21 vol%.

The injection process was performed using an injection molding machine (DSM Xplore Injection Molding). Injection temperature should have a higher melting point than the binder to ensure that feedstock can be filled into the cavity completely. The mold temperature should be close to the melting point of the binder to induce the filling process. Moreover, the mold should be heated to avoid transfer of a large gradient of heat from feedstock to the mold. The melting points of palm stearin and polyethylene were determined through Differential Scanning Calorimetry [19]. Some defects such as a short shot typically occur with less pressure.

Table 1
Distribution of particle size for HA and Ti6Al4V powders.

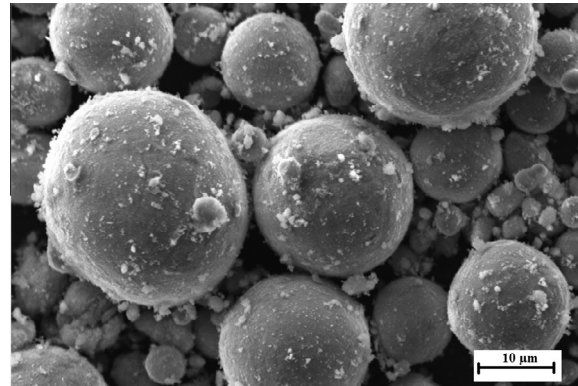| Powder type	D_{10} (μm)	D_{50} (μm)	D_{90} (μm)
HA	2.3	5.3	22.3
Ti6Al4V	10.3	19.6	32.1

Fig. 2. SEM image of the powder mixture of Ti6Al4V and HA after pre-mixing.

A series of trial and error tests were conducted to determine the optimal values of the parameters in the process. The values for melt temperature, mold temperature, and injection pressure were set at 160 °C, 100 °C, and 10 bar, respectively, which are the optimal values to produce green part without any defect in this experiment.

The binder was removed through thermal debinding under argon flow, and sintering is performed under vacuum condition. Thermal debinding was performed in two stages: a 3 °C/min ramp to 320 °C for 1 h; and a 5 °C/min ramp to 500 °C for 1 h. Slow heating rate was employed in the initial stage to remove palm stearin and to avoid defect. Holding temperature for thermal debinding was determined by the TGA curve of both binders. Palm stearin and polyethylene decompose at temperatures above 300 and 450 °C, respectively [19]. The debound part was sintered at 1100, 1200, and 1300 °C in a high-vacuum furnace for 2 h.

The mechanical properties of the sintered HA/Ti6Al4V composite were analyzed using INSTRON 5567, an Instron universal test machine based on MPIF standard 41 [22]. Scanning electron microscopy (SEM) and X-ray diffraction (XRD) were used to study the surface morphology and material phases, respectively. EDS mapping was used to analyze the concentration and distribution of ions on the sintered part.

In vitro test was conducted to analyze the biocompatibility of the sintered part of HA/Ti6Al4V composite. The sintered parts were immersed in the simulated body fluid (SBF) solution based on Kokubo method [23]. The samples were immersed for 1, 2, 6, and 8 weeks and their weight was measured at each time point.
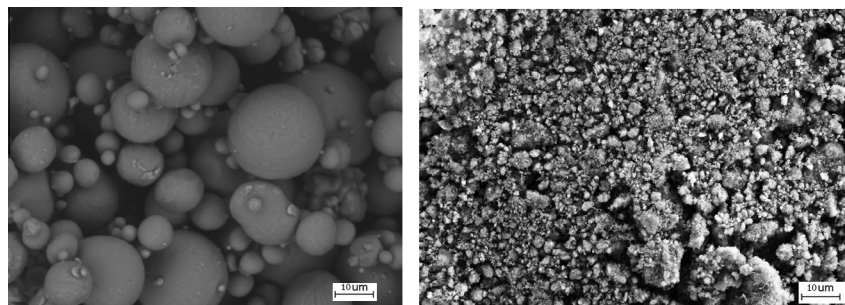

Fig. 1. SEM image of the (a) Ti6Al4V powder and (b) HA powder.

3. Results and discussion

The viscosity–shear rate graphs for all of the feedstock derived in rheological result are shown in Fig. 3. In general, the viscosities of feedstock decrease with increasing shear rate, which indicates pseudoplastic behavior. The behavior of feedstock was calculated according to the following power law Eq. (1).

$$\eta = K\gamma^{n-1} \tag{1}$$

where η and K are the flow behavior indexes for viscosity and constant [24].

The feedstock with pseudoplastic behavior has an n value less than 1, whereas the feedstock with $n = 1$ is called Newtonian [24,25]. Based on the power law, an exponent n ranging from 0.09 to 0.21 indicates a pseudoplastic behavior of the feedstock. The flow behavior index value for 140, 160, and 180 °C are 0.21, 0.09 and 0.15, respectively. The measured viscosity and shear rate are 100–600 Pa s and 1000–6000 s^{-1}, respectively; however, the injectable range of feedstock for PIM ranged from $10^2 \, s^{-1}$ to $10^5 \, s^{-1}$ for shear rate and below 10^3 Pa s for viscosity [3]. Powder characteristics and binder composition are important in determining feedstock behavior [25,26]. According to German and Bose [3], the feedstock for injection molding application should be in pseudoplastic condition; although, in another study [19], dilatant condition is considered injectable.

Fig. 4 shows the shrinkage of the sintered part at every sintering temperature. The shrinkage of the sintered part increases with increasing sintering temperature. The largest shrinkage is 3.07% compared to dimension of green part, which occurred at the highest sintering temperature 1300 °C, whereas the lowest shrinkage (1.87%) occurred at the lowest sintering temperature 1100 °C. The high sintering temperature cause diffusion rate of Ti increases and induces densification particle [27]. At high sintering temperatures, HA is unstable and decomposes to secondary phase [28,29]. At sintering temperature of 1300 °C, HA partially decomposed and Ti ion easily diffused. Thian et al. reported that the presence of HA blocks the diffusion of Ti atoms [12]. Utilization of high vacuum is also a significant contributor in accelerating the decomposition of HA and shrinkage of the sintered part. Fig. 5 shows the physical changes of HA/Ti6Al4V composite at green, brown and sintered part. The densification of titanium significantly reduced the size of the sintered part. In order to clarify shrinkage in quantitative, Table 2 shows variation of dimension in term of width, thickness and length of green, brown and sintered part, respectively. Table 2 indicates that shrinkages of sintered part in thickness, width and length direction.
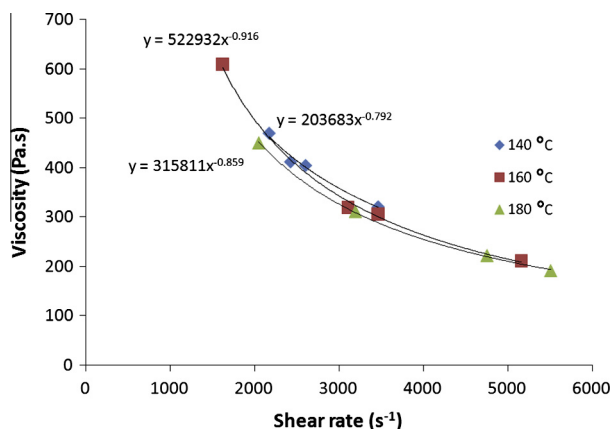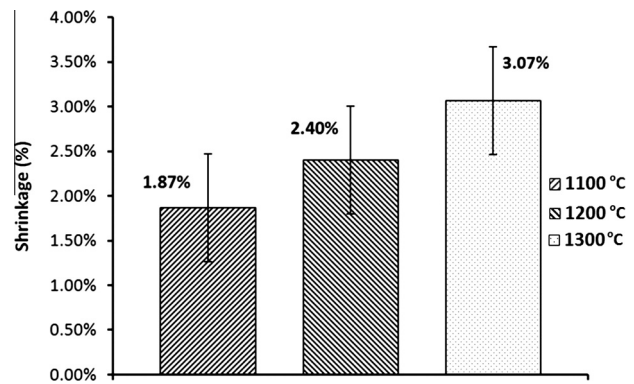
Fig. 4. Effect of sintering temperature on the shrinkage of HA/Ti6Al4V composite.
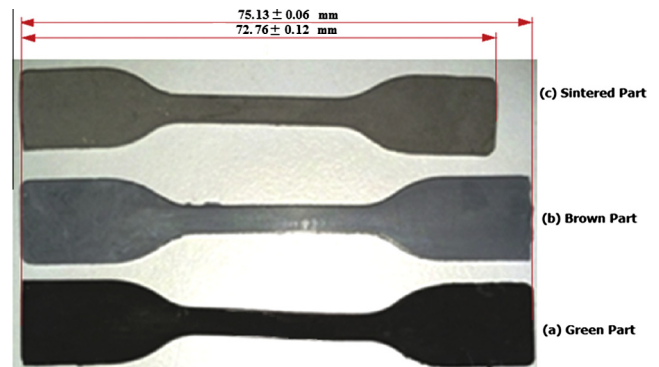
Fig. 5. Physical changes of the HA/Ti6Al4V composite at different stages; (a) green part, (b) brown part, and (c) sintered part, at sintering temperature of 1300 °C. (For interpretation of the references to colour in this figure legend, the reader is referred to the web version of this article.)

Fig. 6 shows the effects of sintering temperature on the flexural strength and the Young's modulus of the HA/Ti6Al4V composite. The strength tends to increase with sintering temperature from 67.12 MPa to 112.97 MPa. The maximum flexural strength was achieved at high sintering temperature 1300 °C and minimum flexural strength at sintering temperature 1100 °C as shown Fig. 6a. A reliable explanation for this trend is the increasing ion diffusion, which encourages powder densification [30].

Young's modulus is one of the criteria for human bone implants, which should be from 10 GPa to 30 GPa depending on the bone position [9]. Fig. 6b shows the Young's modulus of HA/Ti6Al4V in various sintering temperatures. The Young's modulus stabilizes and increases at temperatures above 1300 °C. Sintering temperature is a significant parameter in increasing the flexural strength and the Young's modulus of HA and Ti composites [12]. Fig. 7 shows the surface micrograph of the samples at different processing stages in PIM. The binder system fills the gap among the particles and covers the surface of specimen (Fig. 7a). The binder system acts as a binder and a lubricant to facilitate removal of the surfactant and the specimen from the mold [3]. The binder system was successfully removed using thermal debinding, as shown in Fig. 7b; palm stearin and PE are removed separately in the first and second stages. The HA decomposes and forms a secondary phase, which tends to cover the titanium particles (Fig. 7c). The presence of HA prevented the diffusion of titanium particles and held the shape of the titanium particles. The precipitation of calcium phosphate on the surface of the titanium particles in the early stage is promoted by the dissolution of the secondary phase of HA [12]. The titanium particles formed a neck for diffusion in an area with low concentration of calcium phosphate precipitation. The decomposition of HA left pores on the sintered part as shown on

Fig. 3. Variation of viscosity against shear rate at various temperature.

Table 2
Shrinkage of HA/Ti6Al4V composite at green, brown and sintered part.

Green part (mm)			Brown part (mm)			Sintered part (mm)		
Width	Thickness	Length	Width	Thickness	Length	Width	Thickness	Length
4.07 ± 0.03	2.11 ± 0.05	75.13 ± 0.06	4.04 ± 0.02	2.04 ± 0.02	75.12 ± 0.03	3.99 ± 0.01	2.00 ± 0.01	72.76 ± 0.12
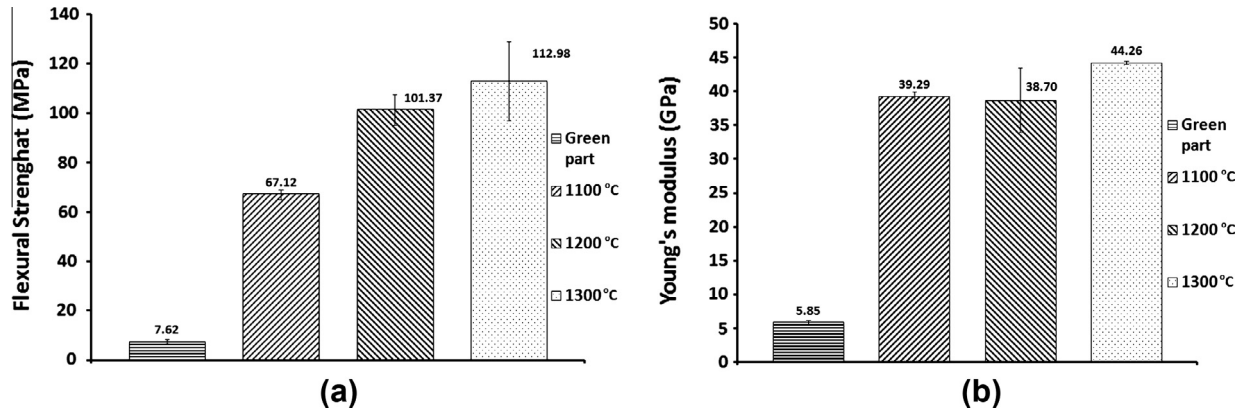
Fig. 6. Effect of sintering temperature on (a) flexural strength of HA/Ti6Al4V composite and (b) Young's modulus of HA/Ti6Al4V composites.
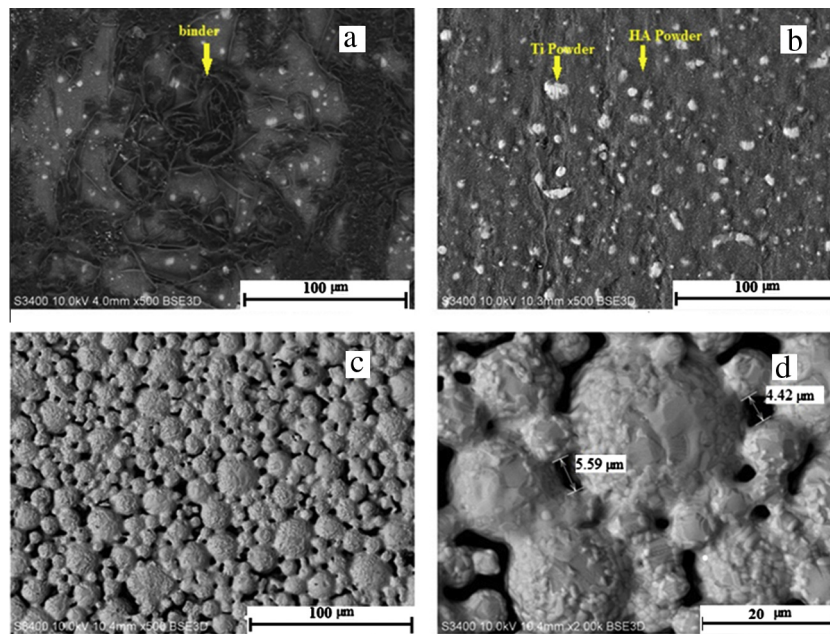
Fig. 7. SEM micrographs of the microstructural changes during PIM stages; (a) green part, (b) brown part, (c) sintered part, and (d) magnification sintered part(c) at 2000×. (For interpretation of the references to colour in this figure legend, the reader is referred to the web version of this article.)

the Fig. 7d. The decomposition of HA occurred in each sintering temperature, and the decomposition rate tend to increase at high sintering temperature. In this case, HA behaves like a space holder. The HA/Ti6Al4 structure (Fig. 7c and d) is fully supported by the titanium alloy with a necking formation, whereas HA decomposed into a secondary phase, which has small contribution to the stability structure of the composite.

Fig. 8 shows the sintered part in various temperatures. Residual HA particles are found in the gap between titanium particles, and HA partially decomposed and covered the titanium particles. At sintering temperature of 1100 °C, some groups of HA are found on the surface, which are absent at relatively higher sintering temperatures. The presence of titanium atom accelerates HA dehydroxylation and titanium oxide formation [6,31]. The use of high

vacuum is believed to be a significant factor in inducing the dehydroxylation rate of HA. Inter-diffusion occurred on the interface of titanium and HA, and titanium atom migrated to the HA and oxygen atoms as HA moved to the titanium bulk. Oxygen as interstitial atom diffused to Ti lattice until saturation, followed by the oxidation of titanium, which decelerated the oxygen diffusion.

Fig. 9 shows the cross-section of the HA/Ti6Al4V composite after grinding and polishing. Based on the EDS mapping results, high concentration of titanium, aluminum, and vanadium ions are spread completely in the composite. Ratio Ca/P is an important factor in determining the properties of calcium phosphate. HA indicated a Ca/P ratio of 1.65, which is higher than that of calcium phosphate. At high sintering temperature, HA is unstable and decomposes to a secondary phase. Phosphorus ions are highly
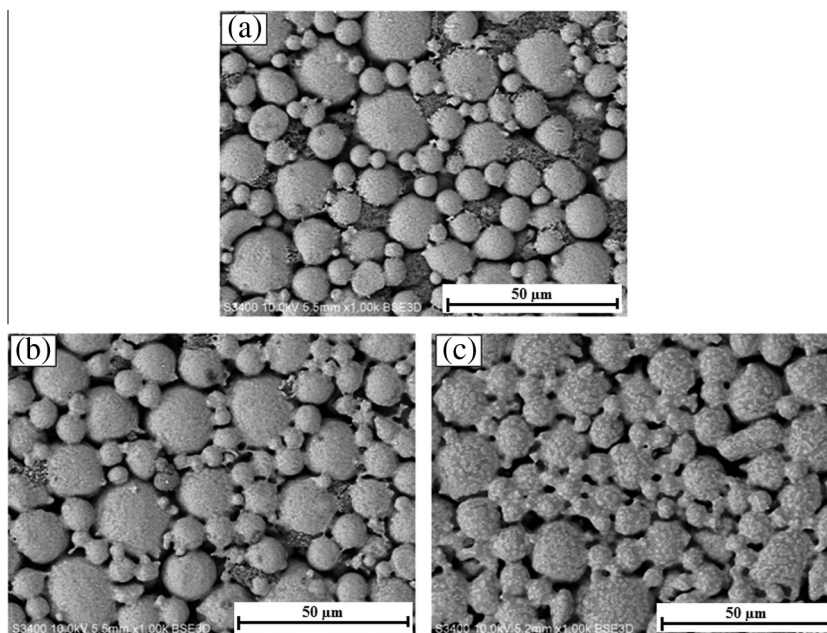
Fig. 8. Surface morphology of sintered parts at various sintering temperatures at (a) 1100 °C, (b) 1200 °C, and (c) 1300 °C with 2 h holding time.
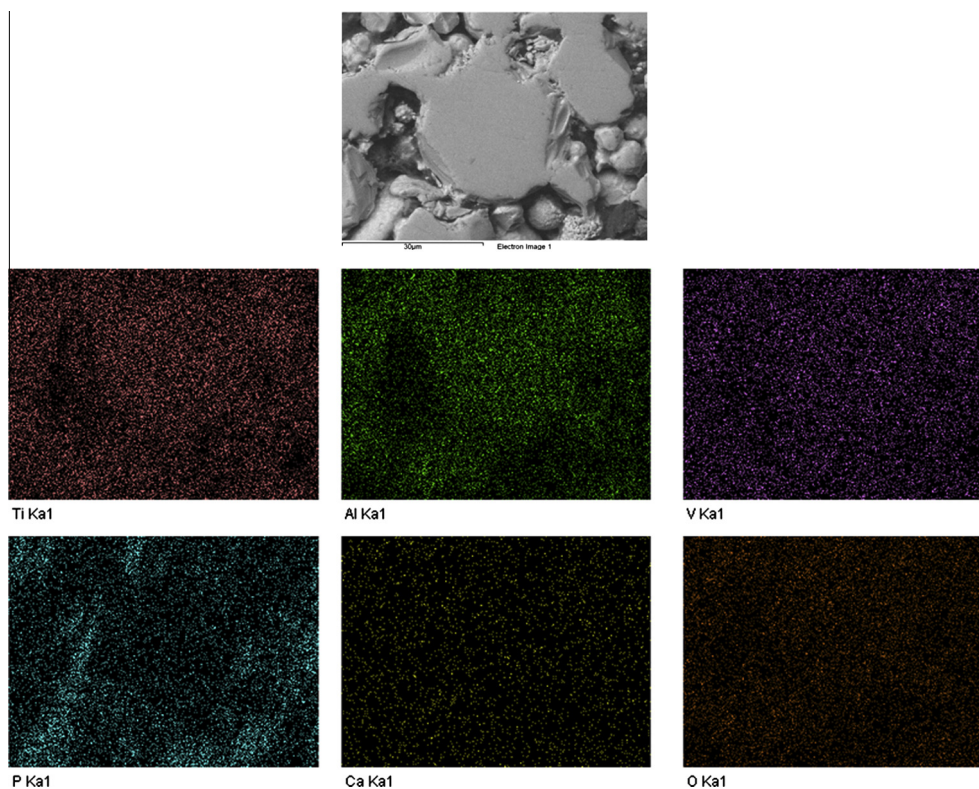

Fig. 9. Variation EDS mapping of the HA/Ti6Al4V composite at sintering temperature 1200 °C.

concentrated on the surface of the titanium particles, and then migrate to the middle position of the titanium particles. Phosphorous ion has small radius and low activation energy, which facilitates easy diffusion in the bulk titanium alloy [9]. Homogenous oxygen and calcium ion distributions are observed because of the low atomic diameter of the oxygen ion.

Fig. 10 shows the XRD patterns for the feedstock powder mixture and composites sintered at 1100, 1200, and 1300 °C. Raw powder is a control powder that comprises HA and titanium powders. The XRD patterns showed the combination of HA spectrum (JCPDS 00-009-0432 card) and titanium (JCPDS 00-001-1198 Card). Some of the phases observed in the sintered part are TiO (JCPDS 00-012-0754), TiC (JSPDS 00-032-1383 card), and β-TCP (JSPDS 00-009-0169 card). In all of the sintering temperature, the XRD patterns of the HA/Ti6Al4V samples did not show the main peak of HA, which suggests that HA was decomposed. Moreover, in each sintering temperature, titanium oxide phases are observed, resulting from the interaction of Ti with O ions from
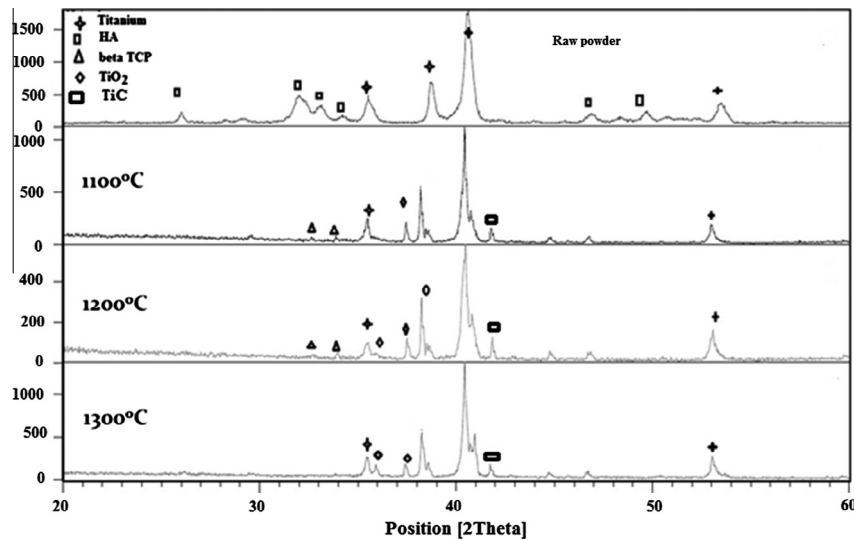
Fig. 10. XRD patterns of feedstock powder mixture and HA/Ti6Al4V composites sintered at 1100, 1200, and 1300 °C.
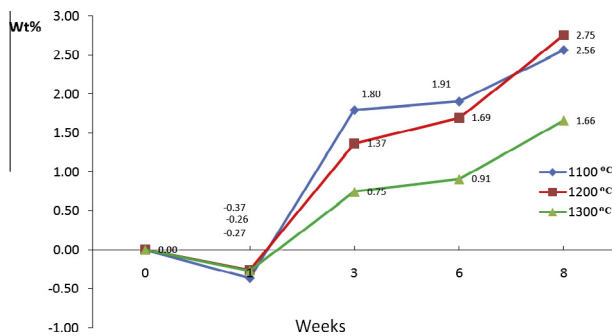

Fig. 11. Weight changes of the sintered HA/Ti6Al4V composites during eight weeks.

the bulk HA. These phase formations is a common phase of interaction between HA and Ti, as reported [11,12]. HA underwent gradual decomposition especially at sintering temperature of

1300 °C. The mechanical properties of the HA/Ti6Al4V composite improve with increasing sintering temperature, however, bioactivity and biocompatibility should still be considered.

Fig. 11 shows the weight changes of the samples sintered at 1100, 1200, and 1300 °C after immersion in SBF for eight weeks. The decomposition rate of HA at high temperature increase; that is, the amount of HA phase varies in every sintering temperature. Ning and Zhou [32] reported that the composition of HA in HA/Ti composite determines the bioactivity level of the material. As shown in Fig. 11, the weight of the sintered part at 1100 and 1200 °C is higher than that at 1300 °C, which illustrates the vital role of HA in increasing the bioactivity of titanium. Moreover, all of the sintered parts lost weight (0.27–0.37%) during the first week. The sintered part at 1100 °C lost the most weight compared with the other samples. The weight loss of the samples in the early stage is attributed to the dissolution of calcium ions from secondary phase after the sintering process [33]. After the gradual decrease in weight of the samples during the first week, the weights of
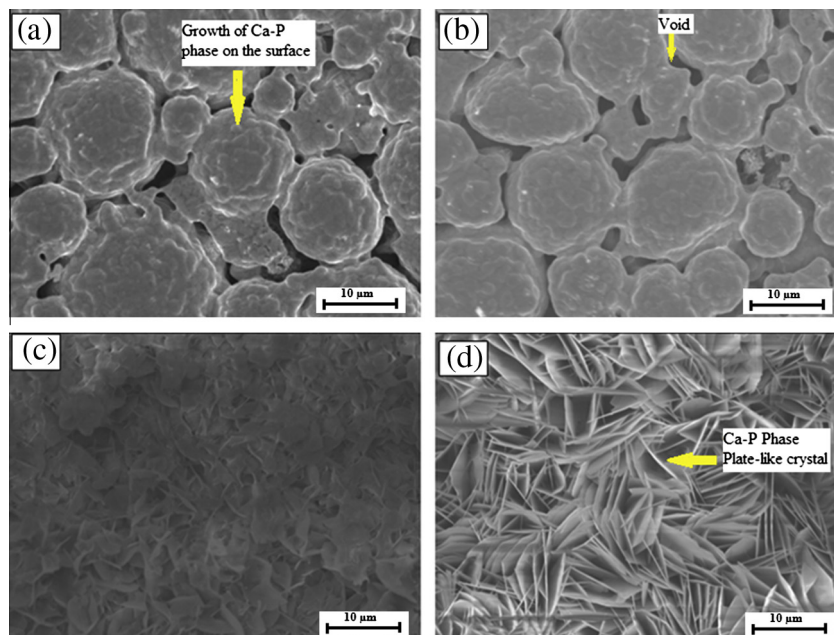

Fig. 12. Morphological changes of the sintered part of HA/Ti6Al4V after immersion in SBF solution after (a) 1, (b) 3, (c) 6 and (d) 8 weeks.

the samples increase significantly, indicating the start of the Ca–P precipitation. This trend is supported by Thian et al., who performed *in vitro* test for Ti6Al4V/HA part using PIM via a ceramic slurry approach with 50 vol% HA [33].

Fig. 12 shows the morphological changes in the sintered HA/Ti6Al4V after immersion in SBF solution after (a) 1, (b) 3, (c) 6, and (d) 8 weeks. Fig. 12(a) shows the condition of the microstructure after one week, as well as the nucleation and growth of Ca–P phase on the Ti particle surface. After three weeks, the size of the Ti particles enlarged because of the growth of the Ca–P phase. After six and eight weeks, the morphology of the sintered part displayed a Ca–P phase layer with plate-like crystal. The precipitation process started with the formation of calcium titanate on the surface of the titanium particle. Precipitation continued with the formation of calcium and phosphate on the calcium titanate, facilitated the formation of an amorphous calcium phosphate layer [11,34]. The morphology of the Ca–P phase during the *in vitro* test using SBF solution is described by Gemelli et al. as a plate-like crystal [34]. Other references reported the titanium oxide phase as a secondary result of the HA–Ti interaction, which is important in the formation of apatite *in vitro* [32]. Although the amount of HA partially decomposed, the HA/Ti6Al4V composite can still be bioactive because of the formation of the titanium oxide induced by the HA–Ti interaction and other secondary phases.

4. Conclusions

In summary, HA/Ti6Al4V composite with a composition of 90 wt% Ti6Al4V and 10 wt% HA was successfully fabricated via PIM. Palm stearin was used as binder for the HA/Ti6Al4V composite. Moreover, rheological results revealed that the HA/Ti6Al4V powder with binder system (PE and palm stearin) showed pseudoplastic behavior within the viscosity of 100–600 Pa s and shear rate of 1000–6000 s^{-1}, thereby indicating affirms the suitability of PIM for fabricating the HA/Ti6Al4V composite. Isotropic micro porous was clearly observed on the sintered composites because of the HA decomposition. The composite sintered at 1300 °C showed the maximum shrinkage of 3.16% with respect to the mold, as well as the best mechanical properties (flexural strength of 112.97 MPa and Young's modulus of 44.26 GPa). The decomposition rates of HA increase with the increasing in sintering temperature. Moreover, the dissolution of HA was observed on the surface of the titanium particles. Based on *in vitro* test using SBF, the sintered HA/Ti6Al4V composite showed induces nucleation and growth of Ca–P phase on the surface of the Ti particles. In addition, even though the HA phases decomposed and formed a secondary phase, which still endowed for increasing the biocompatibility of the Ti6Al4V.

References

[1] Karataş Ç, Sözen A, Arcaklioglu E, Erguney S. Investigation of mouldability for feedstocks used powder injection moulding. Mater Des 2008;29:1713–24.
[2] Heaney D, Gurosik J, Binet C. Isotropic forming of porous structures via metal injection molding. J Mater Sci 2005;40:973–81.
[3] German RM, Bose A. Injection molding of metals and ceramics. Metal Powder Industries Federation; 1997.
[4] Niespodziana K, Jurczyk K, Jakubowicz J, Jurczyk M. Fabrication and properties of titanium–hydroxyapatite nanocomposites. Mater Chem Phys 2010;123:160–5.
[5] Chu CL, Xue XY, Zhu JC, Yin ZD. Mechanical and biological properties of hydroxyapatite reinforced with 40 vol% titanium particles for use as hard tissue replacement. J Mater Sci – Mater Med 2004;15:665–70.
[6] Chu C, Lin P, Dong Y, Xue X, Zhu J, Yin Z. Fabrication and characterization of hydroxyapatite reinforced with 20 vol% Ti particles for use as hard tissue replacement. J Mater Sci – Mater Med 2002;13:985–92.
[7] Ramesh S, Tan CY, Tolouei R, Amiriyan M, Purbolaksono J, Sopyan I, et al. Sintering behavior of hydroxyapatite prepared from different routes. Mater Des 2012;34:148–54.
[8] Younesi D, Mehravaran R, Akbarian S, Younesi M. Fabrication of the new structure high toughness PP/HA-PP sandwich nano-composites by rolling process. Mater Des 2013;43:549–59.
[9] Arifin A, Sulong AB, Muhamad N, Syarif J, Ramli MI. Material processing of hydroxyapatite and titanium alloy (HA/Ti) composite as implant materials using powder metallurgy: a review. Mater Des 2014;55:165–75.
[10] Jurczyk M, Jurczyk K, Niespodziana K. The manufacturing of titanium–hydroxyapatite nanocomposites for bone implant applications. Nanopages 2006;1:219–29.
[11] Balbinotti P, Gemelli E, Buerger G, de Lima SA, de Jesus J, Camargo NHA, et al. Microstructure development on sintered Ti/HA biocomposites produced by powder metallurgy. Mater Res – Ibero-Am J 2011;14:384–93.
[12] Thian ES, Loh NH, Khor KA, Tor SB. Microstructures and mechanical properties of powder injection molded Ti–6Al–4V HA powder. Biomaterials 2002;23:2927–38.
[13] Pattanayak D, Rao BT, Mohan TRR. Calcium phosphate bioceramics and bioceramic composites. J Sol–Gel Sci Technol 2011;59:432–47.
[14] Leyens C, Peters M. Titanium and titanium alloys. John Wiley & Sons; 2006.
[15] Niinomi M. Mechanical biocompatibilities of titanium alloys for biomedical applications. J Mech Behav Biomed 2008;1:30–42.
[16] Ryan G, Pandit A, Apatsidis DP. Fabrication methods of porous metals for use in orthopaedic applications. Biomaterials 2006;27:2651–70.
[17] Oh I-H, Nomura N, Masahashi N, Hanada S. Mechanical properties of porous titanium compacts prepared by powder sintering. Scr Mater 2003;49:1197–202.
[18] Arifin A, Sulong AB, Muhamad N, Syarif J, Ramli MI. HA/Ti6Al4V powder with palm stearin binder system – feedstock characterization. Appl Mech Mater 2014;564:372–5.
[19] Mohd Foudzi F, Muhamad N, Sulong AB, Zakaria H. Yttria stabilized zirconia formed by micro ceramic injection molding: rheological properties and debinding effects on the sintered part. Ceram Int 2013;39:2665–74.
[20] Ramli MI, Sulong AB, Arifin A, Muchtar A, Muhamad N. Powder injection molding of SS316L/HA composite: rheological properties and mechanical properties of the green part. J Appl Sci Res 2012;8(11):5317–21.
[21] Nor NHM, Muhamad N, Ibrahim MHI, Ruzi M, Jamaludin KR. Optimization of injection molding parameter of Ti–6Al–4V powder mix with palm stearin and polyethylene for the highest green strength by using Taguchi method. Int J Mech Mater Eng 2011;6(1):126–32.
[22] MPIF. Standard test methods for metal powders and powder metallurgy products. Determination of transverse rupture strength of powder metallurgy materials. Princeton (NJ): Metal Powder Industries Federation; 2006.
[23] Kokubo T, Takadama H. How useful is SBF in predicting in vivo bone bioactivity? Biomaterials 2006;27:2907–15.
[24] Huang B, Liang S, Qu X. The rheology of metal injection molding. J Mater Process Technol 2003;137:132–7.
[25] Ahn S, Park SJ, Lee S, Atre SV, German RM. Effect of powders and binders on material properties and molding parameters in iron and stainless steel powder injection molding process. Powder Technol 2009;193:162–9.
[26] Hausnerova B. Rheological characterization of powder injection molding compounds. Polimery W 2010;55:3–11.
[27] Heaney DF, Spina R. Numerical analysis of debinding and sintering of MIM parts. J Mater Process Technol 2007;191:385–9.
[28] Ruys AJ, Wei M, Sorrell CC, Dickson MR, Brandwood A, Milthorpe BK. Sintering effects on the strength of hydroxyapatite. Biomaterials 1995;16:409–15.
[29] Tõnsuaadu K, Gross KA, Plūduma L, Veiderma M. A review on the thermal stability of calcium apatites. J Therm Anal Calorim 2011;110:647–59.
[30] Kang SJ. Sintering: densification, grain growth, and microstructure. Oxford: Butterworth-Heinemann; 2005.
[31] Ye H, Liu X, Hong H. Characterization of sintered titanium/hydroxyapatite biocomposite using FTIR spectroscopy. J Mater Sci – Mater Med 2009;20:843–50.
[32] Ning C, Zhou Y. Correlations between the in vitro and in vivo bioactivity of the Ti/HA composites fabricated by a powder metallurgy method. Acta Biomater 2008;4:1944–52.
[33] Thian ES, Loh NH, Khor KA, Tor SB. In vitro behavior of sintered powder injection molded Ti–6Al–4V/HA. J Biomed Mater Res 2002;63:79–87.
[34] Gemelli E, Resende CX, de Almeida Soares GD. Nucleation and growth of octacalcium phosphate on treated titanium by immersion in a simplified simulated body fluid. J Mater Med 2010;21:2035–47.